Hydrogen sulfide inhibits the renal fibrosis of obstructive nephropathy

Kai Song[1,2,6], Fen Wang[1,6], Qian Li[1], Yong-Bing Shi[2], Hui-Fen Zheng[1], Hanjing Peng[3], Hua-Ying Shen[2], Chun-Feng Liu[1,4] and Li-Fang Hu[1,4,5]

[1]Institute of Neuroscience, Soochow University, Suzhou, China; [2]Department of Nephrology, Second Affiliated Hospital of Soochow University, Suzhou, China; [3]Department of Chemistry and Center for Diagnostics and Therapeutics, Georgia State University, Atlanta, Georgia, USA; [4]Department of Neurology, Second Affiliated Hospital of Soochow University, Suzhou, China and [5]Department of Pharmacology, School of Pharmaceutical Science, Soochow University, Suzhou, China

Hydrogen sulfide has recently been found decreased in chronic kidney disease. Here we determined the effect and underlying mechanisms of hydrogen sulfide on a rat model of unilateral ureteral obstruction. Compared with normal rats, obstructive injury decreased the plasma hydrogen sulfide level. Cystathionine-β-synthase, a hydrogen sulfide-producing enzyme, was dramatically reduced in the ureteral obstructed kidney, but another enzyme cystathionine-γ-lyase was increased. A hydrogen sulfide donor (sodium hydrogen sulfide) inhibited renal fibrosis by attenuating the production of collagen, extracellular matrix, and the expression of α-smooth muscle actin. Meanwhile, the infiltration of macrophages and the expression of inflammatory cytokines including interleukin-1β, tumor necrosis factor-α, and monocyte chemoattractant protein-1 in the kidney were also decreased. In cultured kidney fibroblasts, a hydrogen sulfide donor inhibited the cell proliferation by reducing DNA synthesis and downregulating the expressions of proliferation-related proteins including proliferating cell nuclear antigen and c-Myc. Further, the hydrogen sulfide donor blocked the differentiation of quiescent renal fibroblasts to myofibroblasts by inhibiting the transforming growth factor-β1-Smad and mitogen-activated protein kinase signaling pathways. Thus, low doses of hydrogen sulfide or its releasing compounds may have therapeutic potentials in treating chronic kidney disease.

Correspondence: *Chun-Feng Liu, Department of Neurology, Second Affiliated Hospital of Soochow University, 1055 Sanxiang Road, Suzhou 215004, China. E-mail: liucf@suda.edu.cn or Li-Fang Hu, Institute of Neuroscience, Soochow University, 199 Ren-Ai Road, Suzhou Industrial Park, Suzhou 215123, China. E-mail: hulifang@suda.edu.cn*

[6]Fen Wang and Kai Song are co-first authors.

Tubulointerstitial fibrosis is the final common pathway to chronic kidney diseases (CKD).[1] Pathologically, renal fibrosis manifests as the formation of myofibloblasts and the deposition of extracellular matrix proteins in the renal interstitium.[2] The mechanisms of renal fibrosis have not been fully elucidated and effective drugs are still scarce. Renin–angiotensin–aldosterone system is one of the main culprits of renal fibrogenesis, and renin–angiotensin–aldosterone system inhibitors remain the first-line drugs in fighting renal fibrosis.[3] However, the renin–angiotensin–aldosterone system inhibitors may deteriorate renal function and cause hyperpotassemia when serum creatinine rises above 3 mg/dl.[4] New antifibrotic agents are therefore needed to expand therapeutic options and decrease side effects, which is especially important for azotemia patients.

Hydrogen sulfide (H_2S) represents the third gasotransmitter along with nitric oxide and carbon monoxide.[5] It is generated by cystathionine-γ-lyase (CSE), cystathionine-β-synthase (CBS), and 3-mercaptopyruvate sulphurtransferase. CBS and CSE are enriched in renal proximal tubules and produce H_2S in kidney in a combined way.[6] H_2S plays various physiological and pathological roles in the kidney. For instance, it exhibits diuretic, natriuretic, and kaliuretic properties by increasing glomerular filtration rate and functions as an oxygen sensor in the renal medulla.[6,7] Recently, it was reported that plasma H_2S level was decreased in 5/6 nephrectomy rat and uremia patients,[8,9] suggesting that uremic toxin of CKD impairs the production of endogenous H_2S.

Notably, the biological functions of H_2S in CKD are not fully understood. Heterozygous $cbs^{-/-}$ mice with unilateral nephretomy, an animal model of CKD, developed proteinuria and collagen deposition, and increased the expressions of matrix metalloproteinase-2 and -9.[10] Emerging evidence also demonstrates that H_2S exhibits antifibrotic effects in the lung, heart, and liver.[11–13] Furthermore, H_2S bears some similarities to the other two gaseous molecules, nitric oxide and carbon monoxide, both of which protect the kidney from renal fibrosis.[14,15] Taken together, we hypothesize that H_2S may attenuate renal fibrosis.

In this study, we examined the effect of H$_2$S on unilateral ureteral obstructive (UUO) animal model and defined its safe and effective dosage range. Furthermore, we investigated the roles of H$_2$S in renal fibroblast proliferation and differentiation. The potential mechanisms were also explored.

RESULTS

CBS expression and plasma H$_2$S levels are decreased in the obstructed kidney

To investigate whether endogenous H$_2$S was involved in the pathogenesis of renal fibrosis, we examined the expression and activity of H$_2$S-producing enzymes CBS and CSE, as well as plasma H$_2$S levels. The CBS expression was nearly completely ablated by obstructive injury at day 14, whereas CSE was increased. In contrast, the expressions of CBS and CSE in the contralateral kidneys were not affected (Figure 1a–c). Moreover, H$_2$S generation in the obstructed kidneys was dramatically reduced compared with sham-operated rats (Figure 1d). Plasma H$_2$S levels were reduced by $\sim 30\%$ in UUO rats compared with the sham counterparts ($27.5 \pm 4.3\ \mu mol/l$ vs. $39.4 \pm 6.3\ \mu mol/l$, $P = 0.021$, Figure 1e). Immunohistochemistry staining indicated that CBS was predominantly expressed in proximal renal tubules. UUO injury time-dependently reduced CBS expression in the obstructed kidneys without affecting that in the contralateral and sham-operated kidneys (Figure 2a and b). In contrast, CSE was mainly located in renal glomeruli, interstitium, and interlobular arteries of normal rats. UUO injury markedly increased the CSE expression in the interstitium of obstructed kidneys. The CSE expression in the unobstructed kidneys remained unchanged (Figure 2c and d).

NaHS treatment decreases the renal size, increases the cortical thickness, and ameliorates renal function of UUO rats

To assess the effect of exogenous H$_2$S supplement on renal fibrosis, we treated UUO rats with incremental doses of sodium hydrosulfide (NaHS; 5.6, 56, and 560 μg/kg/day) and CSE inhibitor (DL-propargylglycine (PAG), 25 mg/kg/day) via intraperitoneal injection once daily for 3 days before and 2 weeks after UUO injury. The renin–angiotensin–aldosterone system inhibitor enalapril (10 mg/kg/day) was also administrated via intragastria as a positive control. Gross appearance (Figure 2a) and group data (Figure 2b and c) showed that enalapril and NaHS (56 μg/kg/day) reduced the size of the kidney and increased the renal cortical thickness in UUO rats. However, these effects were not observed in the rats treated with NaHS at a higher dose of 560 μg/kg/day or PAG (Figure 3). Compared with UUO rats, NaHS (56 μg/kg/day) decreased serum creatinine levels, whereas PAG increased serum urea nitrogen concentration. There were no differences of serum electrolytes among each group (Supplementary Data and Supplementary Table S1 online).

NaHS attenuates renal tubulointerstitial injury and collagen deposition in renal interstitium

Hematoxylin and eosin staining results indicated that UUO rats exhibited dilated renal tubule, epithelial cells atrophy, interstitial expansion, and increased infiltration of inflammatory
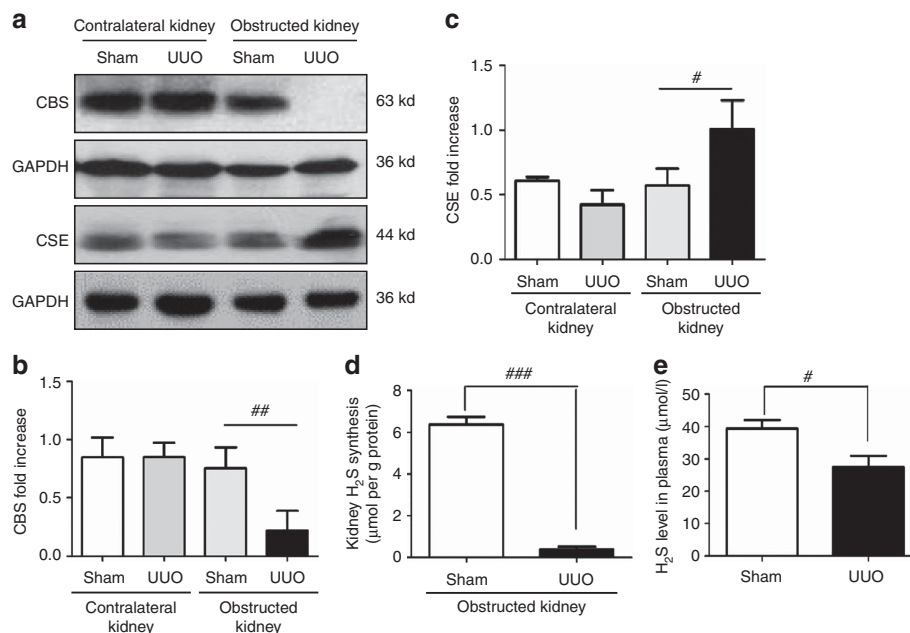

Figure 1 | Unilateral ureteral obstructive (UUO) injury downregulates cystathionine-β-synthase (CBS) expression and decreases hydrogen sulfide (H$_2$S) level in plasma on day 14 after operation. (**a**) Representative western blots of CBS and cystathionine-γ-lyase (CSE) proteins in sham and UUO group are shown. Relative levels of (**b**) CBS and (**c**) CSE were analyzed by normalizing to glyceraldehyde-3-phosphate dehydrogenase (GAPDH). (**d**) Kidney H$_2$S production and (**e**) plasma H$_2$S level in sham and UUO group are shown. Data are mean ± s.e.m., $n = 4$–6, $^{\#}P < 0.05$, $^{\#\#}P < 0.01$, $^{\#\#\#}P < 0.001$ versus sham group.
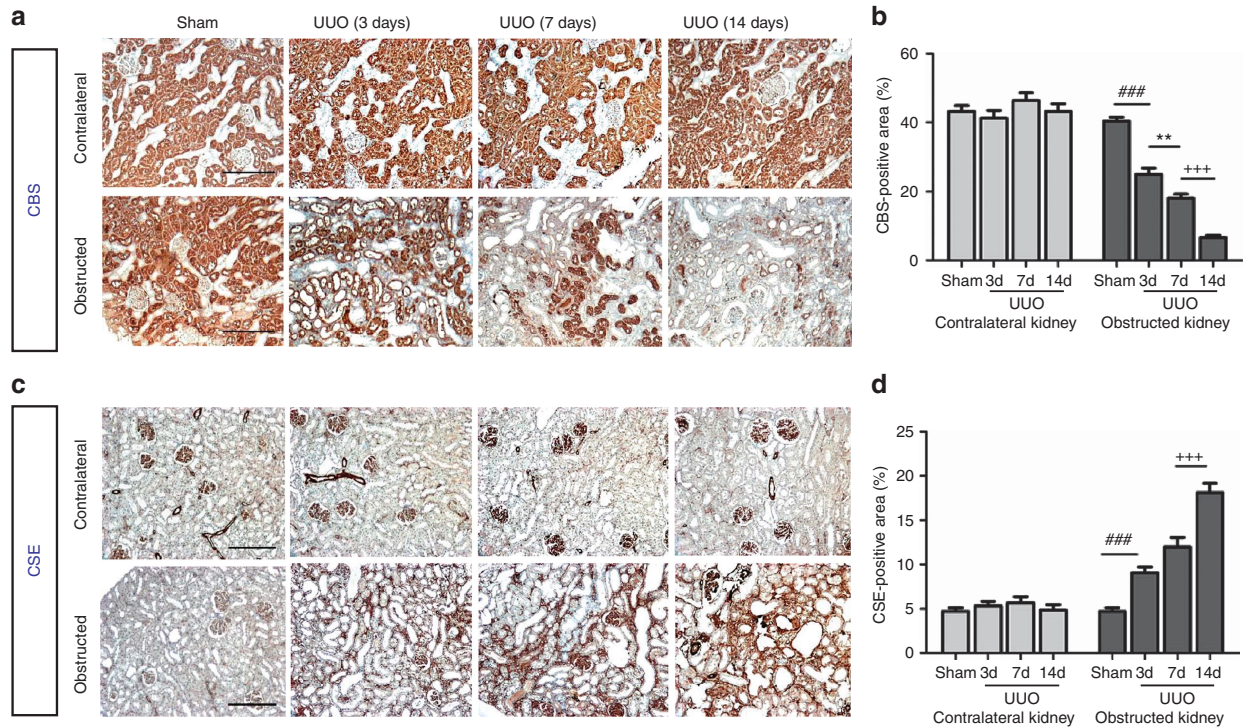
Figure 2 | Expression and localization of cystathionine-β-synthase (CBS) and cystathionine-γ-lyase (CSE) in rat renal cortex after unilateral ureteral obstructive (UUO) injury. (**a**, **b**) CBS was predominantly expressed in proximal renal tubules. CBS expression in the left (obstructed) kidneys was reduced at 3 (3d), 7 (7d), and 14 days (14d) after UUO injury, whereas it remained unchanged in the right (contralateral) kidneys. (**c**, **d**) CSE was mainly located in renal glomeruli, interstitium, and interlobular arteries and was markedly increased in the left (obstructed) kidneys at 3, 7, and 14 days after operation. In contrast, its expression in unobstructed kidneys was not altered. Scale bar = 200 μm. Data are mean ± s.e.m., $n = 4$, $^{###}P < 0.001$ versus sham group, $^{**}P < 0.01$ versus UUO 3-day group, $^{+++}P < 0.001$ versus UUO 7-day group.

cells at 14 days after operation. The tubulointerstitial injury of UUO rats was ameliorated when treated with NaHS (5.6 and 56 μg/kg/day) and enalapril. NaHS at 560 μg/kg/day and PAG failed to ameliorate the tubulointerstitial injury compared with UUO group (Supplementary Data and Supplementary Figure S1 online).

Masson trichrome staining demonstrated that UUO injury resulted in a significant accumulation of collagen fibrils (blue area) compared with the sham group. Enalapril and NaHS (5.6 and 56 μg/kg/day) attenuated the fibrotic lesions with less collagen deposited in the renal interstitium. In contrast, NaHS at 560 μg/kg/day and PAG increased the collagen production compared with that of the UUO group (Figure 4a and b).

NaHS inhibits the expression of SMA and fibronectin in the obstructed kidney

To evaluate whether H₂S reduced the production of myofibroblasts and extracellular matrix, the renal expression of α-smooth muscle actin (α-SMA) and fibronectin were detected on day 14 after UUO operation. Immunohisto-chemistry staining and semiquantitative analysis showed that enalapril and NaHS (5.6 and 56 μg/kg/day) decreased the expressions of α-SMA and fibronectin of the UUO rats. In contrast, NaHS 560 μg/kg/day and PAG increased the

production of these proteins, but statistical difference was not obtained in the PAG group (Figure 5a–d). These observations were verified by western blot analysis, in which NaHS, especially at the dose of 56 μg/kg/day, markedly reduced the expressions of α-SMA, fibronectin, phospho-Smad3, and transforming growth factor-β1 (TGF-β1) (Figure 6a–d).

NaHS inhibits inflammation in the kidney after obstructive injury

The effect of H₂S on the infiltration of inflammatory cells in obstructed kidneys was also determined at 7 days after UUO. CD68 (a macrophage marker) staining in renal cortex revealed an increased macrophage infiltration in the renal interstitium of UUO rats. NaHS (5.6 and 56 μg/kg/day) and enalapril markedly reduced the number of macrophage in the interstitium against the UUO group. This effect was most pronounced in the NaHS (56 μg/kg/d)-treated group. Compared with the UUO group, NaHS at 560 μg/kg/day increased the number of macrophage in renal cortex, whereas PAG tended but failed to significantly increase the CD68-positive cell number (Figure 7a and b).

To confirm the anti-inflammatory effect of NaHS, the mRNA levels of interleukin-1β, tumor necrosis factor-α, and monocyte chemoattractant protein-1 were determined by quantitative PCR. All these inflammatory molecules were
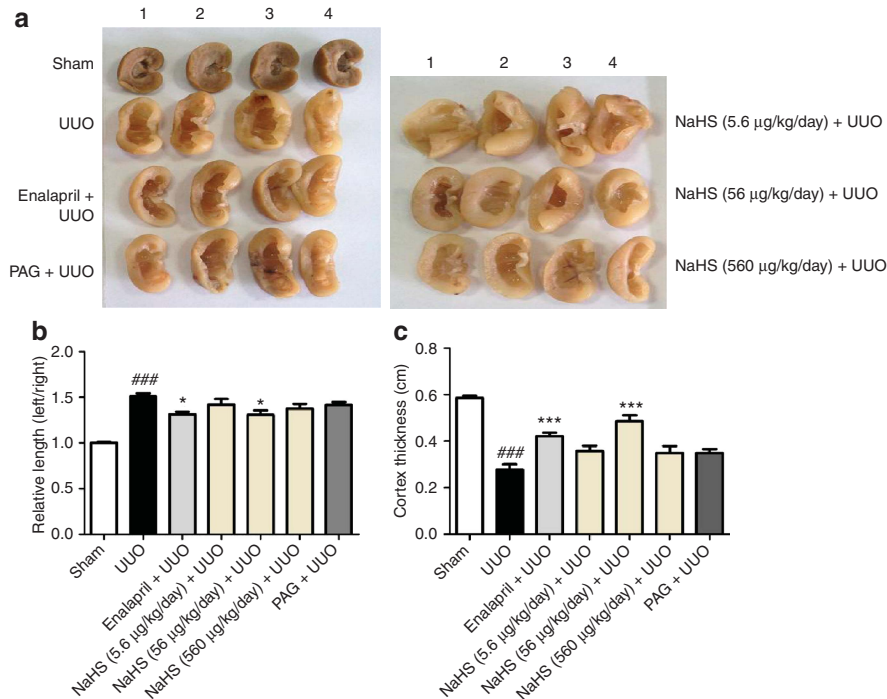
Figure 3 | Sodium hydrosulfide (NaHS) treatment decreases the size and increases the cortical thickness of unilateral ureteral obstructive (UUO) kidney. (**a**) General appearance of four representative left kidneys of rats subjected to various treatments. UUO rats received vehicle (saline) treatment. NaHS (5.6, 56, and 560 μg/kg/day) and DL-propargylglycine (PAG; 25 mg/kg/day) were intraperitoneally given once daily 3 days before and continued for 2 weeks after operation, whereas enalapril (10 mg/kg/day) was given via intragastria. (**b**) Relative lengths of the left kidney calibrated by the right counterpart of the same rat in different groups. (**c**) Renal cortex thickness in the mid-portion of left kidney in coronal section. Data are mean ± s.e.m. ($n = 7$), $^{###}P < 0.001$ versus sham group; $^*P < 0.05$, $^{***}P < 0.001$ versus UUO group.
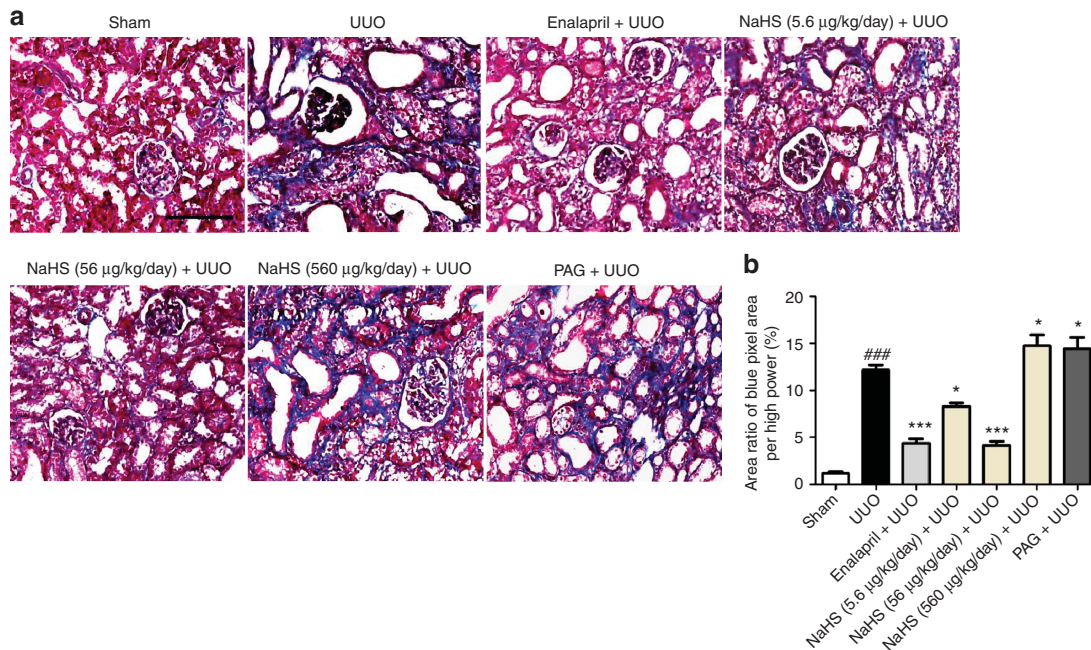

Figure 4 | Sodium hydrosulfide (NaHS) treatment attenuates the accumulation of collagen fibrils in renal interstitium in the obstructed kidneys at 14 days after unilateral ureteral obstructive (UUO) operation. Representative pictures of (**a**) Masson trichrome staining and (**b**) semiquantitative analysis of the proportion with the blue color area over the whole field area in all groups are indicated. PAG, DL-propargylglycine. Scale bar = 200 μm. Mean ± s.e.m. ($n = 4$), $^{###}P < 0.001$ versus sham group; $^*P < 0.05$, $^{***}P < 0.001$ versus UUO group.
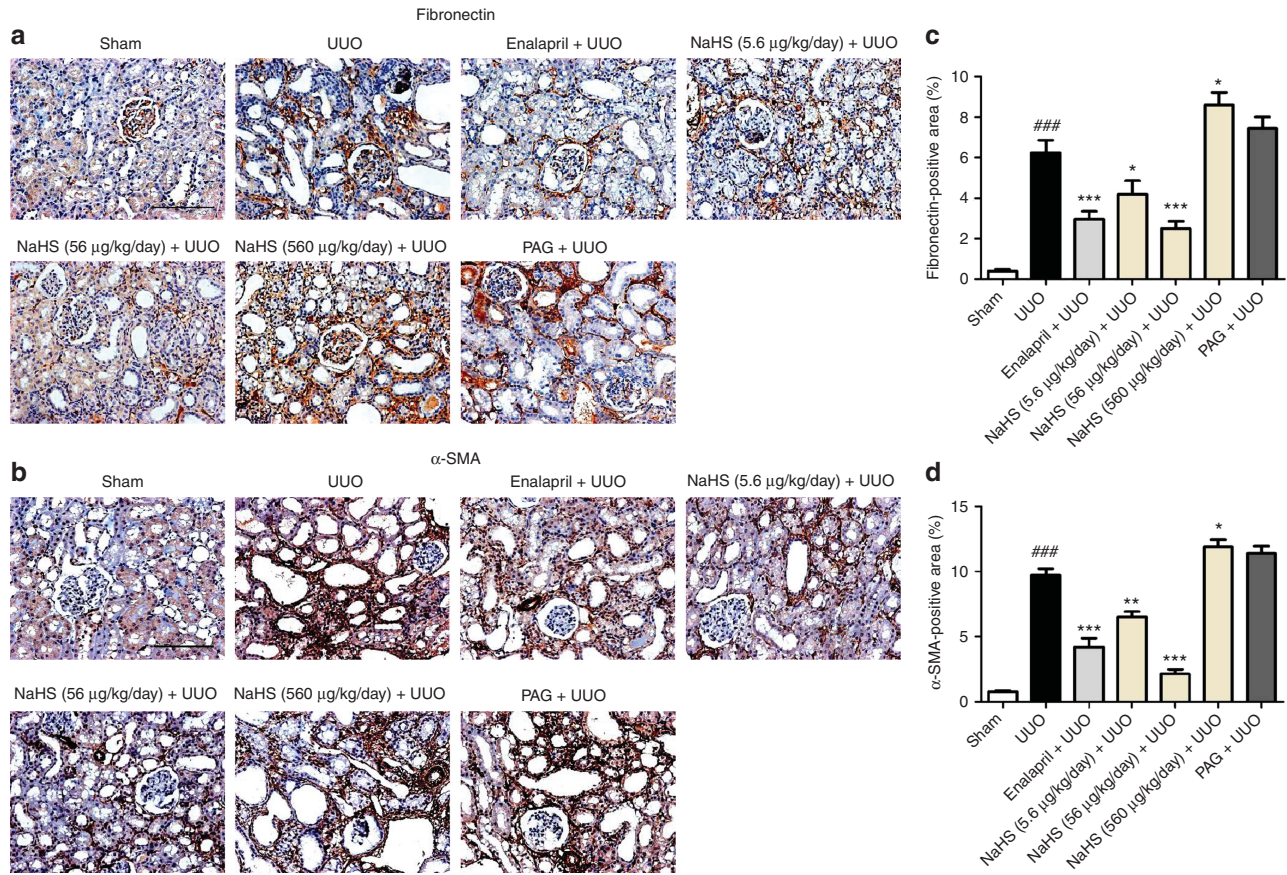
Figure 5 | Sodium hydrosulfide (NaHS) inhibits the expressions of fibronectin and α-smooth muscle actin (α-SMA) in the obstructed kidneys at 14 days after unilateral ureteral obstructive (UUO) operation. Representative immunohistochemistry images for the expression of (**a**) fibronectin and (**b**) α-SMA, and semiquantitative analysis of these two proteins are presented. PAG, DL-propargylglycine. Scale bar = 200 μm. Data are mean ± s.e.m. of 10 non-overlapping fields from four animals per group, [###]$P < 0.001$ versus sham group; [*]$P < 0.05$, [**]$P < 0.01$, [***]$P < 0.001$ versus UUO group.

increased by UUO injury. NaHS (5.6 and 56 μg/kg/day) and enalapril suppressed the expression of these cytokines, whereas NaHS at 560 μg/kg/day and PAG were unable to exhibit anti-inflammatory effects (Figure 7c).

NaHS suppresses the NRK-49F cell proliferation induced by fetal bovine serum (FBS)

We further performed an *in vitro* study to investigate the antiproliferation effect of H₂S on renal fibroblast using NRK-49F cells. Cells were exposed to various concentrations (1–500 μmol/l) of NaHS for 30 min, followed by stimulation with 10% FBS for 24 h. Cells with serum-free medium were set as controls. MTT (3-(4,5-dimethylthiazol-2-yl)-2,5-di-phenyltetrazolium bromide) assay showed the cell number was significantly increased after incubation with 10% FBS for 24 h ($P < 0.05$, Figure 8a). Preincubation with NaHS (10, 50, 100, and 500 μmol/l) reduced the cell number by 17.6%, 14.8%, 21.4%, and 16.2%, respectively. However, statistical difference was only reached in 100 μmol/l NaHS group and the dose-dependent effect was not observed.

Furthermore, we continued to test whether H₂S inhibited the DNA synthesis of renal fibroblast cells using bromodeox-

yuridine (BrdU) incorporation assay. The DNA synthesis triggered by 10% FBS was significantly decreased by NaHS (100 μmol/l) before treatment (Figure 8b and c). To delineate the mechanism beneath the antiproliferation effect of H₂S, the expression of proliferation-related genes, including *proliferating cell nuclear antigen (PCNA)* and *c-Myc*, was also assessed. Preincubation with 100 μmol/l NaHS consistently attenuated the expressions of PCNA and c-Myc proteins induced by 10% FBS stimulation for 24 h (Figure 8d–f).

NaHS blocks the differentiation of quiescent renal fibroblasts to myofibroblasts

Because TGF-β1 is the most potent cytokine controlling the phenotype switch from renal fibroblasts to myofibroblasts, we investigated the effect of H₂S on renal fibroblast activation induced by TGF-β1. Reverse transcription–PCR demonstrated that NaHS pretreatment inhibited the mRNA expressions of collagen I, α-SMA, and fibronectin induced by TGF-β1 (Figure 9a–d). Western blot analysis also revealed a significant elevation of α-SMA and fibronectin expression in NRK-49F cells after TGF-β1 stimulation. These effects were essentially abolished by NaHS (Figure 9e and f).
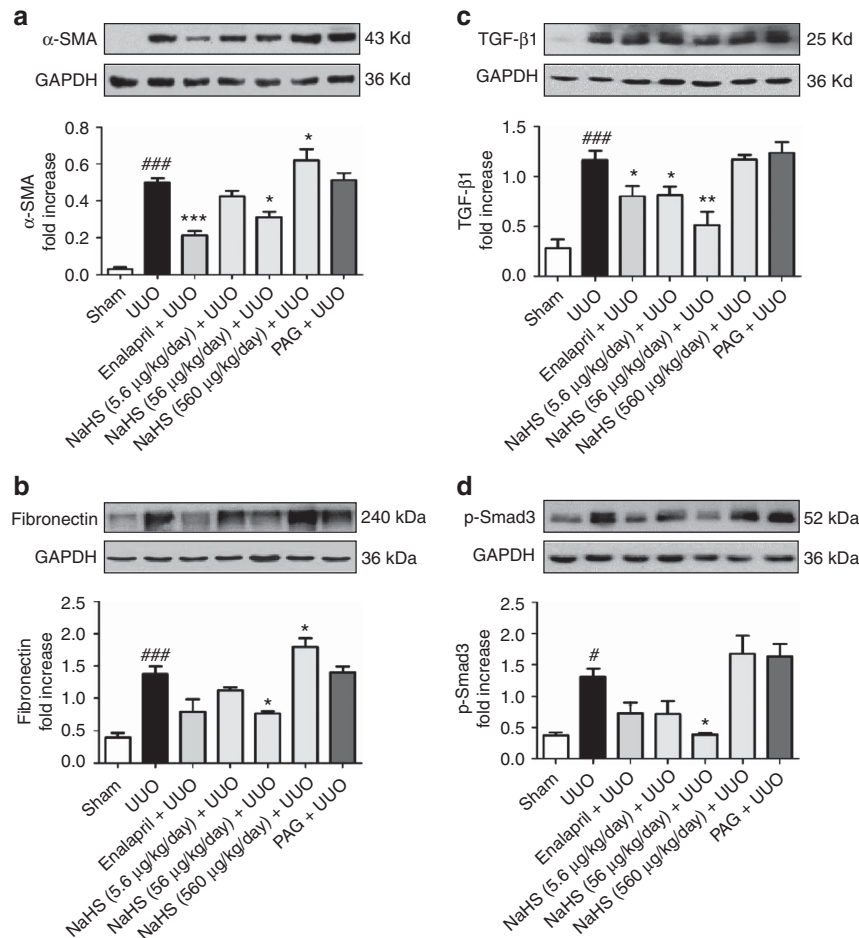
Figure 6 | Sodium hydrosulfide (NaHS) downregulates the expression of fibrosis-associated and signaling molecules in the obstructed kidneys at 7 days after unilateral ureteral obstructive (UUO) operation. Whole kidney tissue lysates were immunoblotted with antibody against (**a**) α-smooth muscle actin (α-SMA), (**b**) fibronectin, (**c**) transforming growth factor-β1 (TGF-β1), and (**d**) phospho-Smad3 in each group and quantitative analyses of the relative abundance of these proteins among various groups are presented. GAPDH, glyceraldehyde-3-phosphate dehydrogenase; PAG, DL-propargylglycine. Mean ± s.e.m., $n = 4$, #$P < 0.05$, ###$P < 0.001$ versus sham group; *$P < 0.05$, **$P < 0.01$, ***$P < 0.001$ versus UUO group.

NaHS abolishes the phosphorylation of the MAPKs and Smad3

TGF-β1-Smad and mitogen-activated protein kinase (MAPK) pathways are two critical signaling mechanisms implicated in renal fibrosis. We therefore examined the effects of H$_2$S on the TGF-β1-induced phosphorylation of Smad3, p38, c-Jun N-terminal kinase (JNK), and extracellular signal–regulated kinase (ERK) with western blot analysis. TGF-β1 (2 ng/ml) triggered the phosphorylation of these proteins with distinct patterns. The phosphorylation of p38 peaked at 0.5 h after TGF-β1 stimulation, quicker than that of the other molecules. Specifically, phosphorylation of ERK and JNK peaked at 2 h after TGF-β1 exposure whereas Smad3 at 1 h (data not shown). Pretreatment with 100 μmol/l NaHS abolished the increase of Smad3 and MAPKs phosphorylation induced by TGF-β1 stimulation (Figure 10).

DISCUSSION

UUO is a well-established animal model featured by progressive renal fibrosis and tubulointerstitial injury. In this

study, we demonstrated that exogenous H$_2$S suppressed collagen and extracellular matrix deposition in the UUO rats. We also identified that H$_2$S blocked renal fibrosis via multiple mechanisms. It inhibited renal fibroblast proliferation by reducing DNA synthesis and downregulating the expressions of proliferation-related proteins. H$_2$S also blocked cell differentiation by suppressing the TGF-β1-Smad and MAPK signal pathways. Besides, H$_2$S inhibited the inflammatory process induced by UUO injury.

The association of H$_2$S and renal fibrosis is not well defined. Our study demonstrated that plasma H$_2$S levels and endogenous H$_2$S production in the obstructed kidneys were decreased in UUO rats. As UUO model is devoid of any exogenous toxin, or a 'uremic' environment,[16] our finding implies that renal fibrosis *per se* could reduce the H$_2$S generation. Our study further demonstrated that CBS was predominantly expressed in renal tubules whereas CSE was mainly located in glomeruli and interstitial vessels, consistent with a recent report.[17] UUO injury markedly decreased the expression of CBS but increased that of CSE in the renal
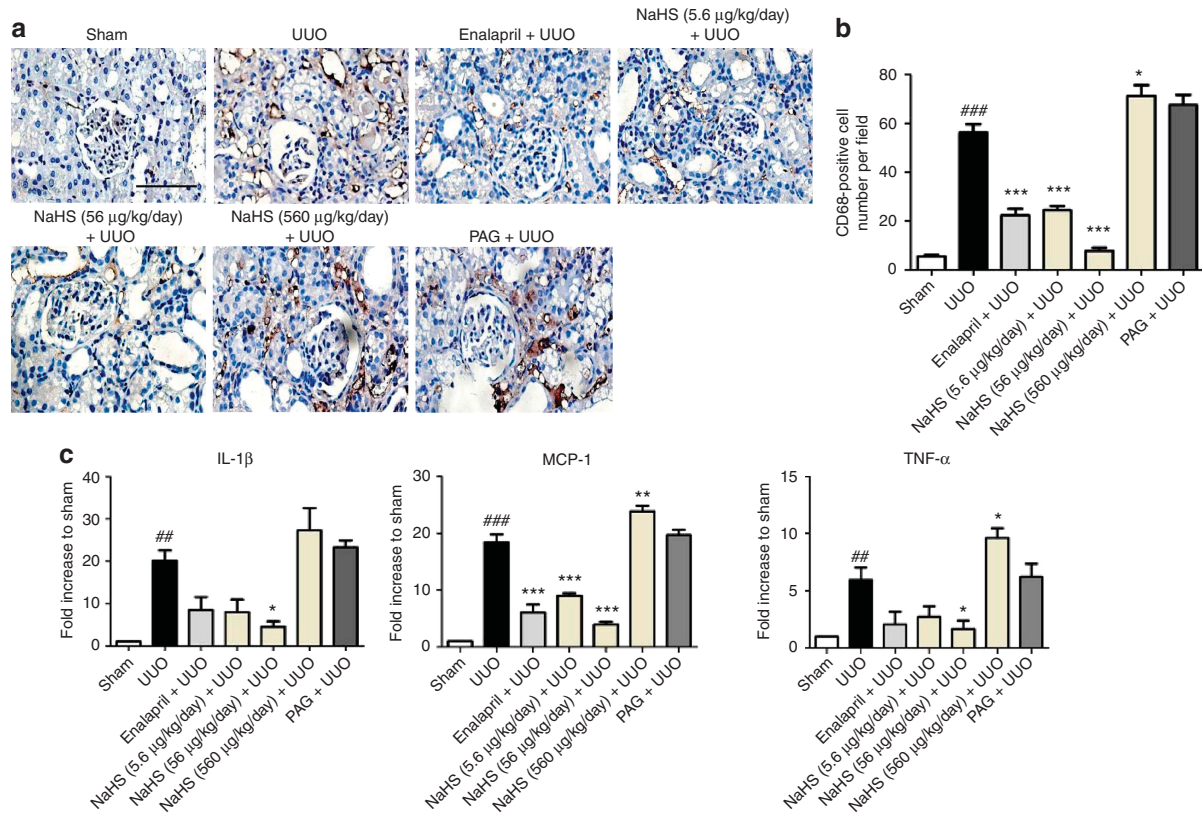
Figure 7 | Sodium hydrosulfide (NaHS) inhibits the macrophage infiltration in the obstructed kidneys at 7 days after unilateral ureteral obstructive (UUO) operation. (**a**) Representative pictures of kidney sections stained with anti-CD68. A total of 10 fields from 4 animals were included in analyzing the number of CD68-positive cells in the interstitium and (**b**) the group data are shown correspondingly. (**c**) Quantitative PCR results of the mRNA levels of interleukin-1β (IL-1β), tumor necrosis factor-α (TNF-α), and monocyte chemoattractant protein-1 (MCP-1) in the kidneys among different treatment groups. PAG, DL-propargylglycine. Scale bar = 100 μm. Data are presented as mean ± s.e.m., $^{\#\#}P<0.01$, $^{\#\#\#}P<0.001$ versus sham group; $^{*}P<0.05$, $^{**}P<0.01$, $^{***}P<0.001$ versus UUO group.

interstitium. This finding is consistent with previous studies that CBS is more predisposed to decrease in kidney disease compared with CSE. For instance, CBS was decreased 6 weeks earlier than CSE in rat remnant kidney.[8] In renal ischemic–reperfusion rats, CBS was reduced as earlier as 6 h after reperfusion,[18] whereas CSE was increased by prolonged reperfusion for 24 h.[19] Hence, the increase of CSE observed in this study could be explained as a 'compensatory mechanism' to maintain the H₂S level. As CSE is abundant in glomeruli, H₂S may also be beneficial for glomerular diseases. A recent study by Lee *et al.*[20] confirms this notion that H₂S is able to protect the renal glomerular epithelial cells from high glucose–induced injury, indicating the reduction of H₂S is involved in diabetic nephropathy.

As the endogenous H₂S production was reduced by UUO injury, it is logical to hypothesize that exogenous H₂S supplementation could relieve renal fibrosis. We observed that the antifibrotic effect of NaHS started at 5.6 μg/kg/day, peaked at 56 μg/kg/day, but was reversed at 560 μg/kg/day. Our results were in line with a prior study in which the most effective NaHS dose on cardiac ischemia–reperfusion injury was 56 μg/kg/day.[21] Moreover, low doses of NaHS (78 and 392 μg/kg/day body weight, twice daily) also reduced

pulmonary fibrosis induced by bleomycin.[11] Previous studies demonstrated that H₂S level in vertebrate blood varied from 10–300 μmol/l by the methylene blue assay.[22,23] Using a sensitive fluorescent probe,[24] we found the plasma H₂S level in normal rat was ∼30–40 μmol/l, whereas its counterpart in the UUO rat was 20–30 μmol/l. Nevertheless, the precise determination of H₂S in biological samples is still controversial. More sensitive techniques such as monobromobimane-based assay and quantum dot/nanoparticle methods recently indicated that blood and tissue H₂S concentrations were as low as 0.15–0.9 μmol/l.[25,26] These findings may justify the application of H₂S at relatively low doses in treating renal fibrosis.

Although H₂S is beneficial in most animal models of renal diseases, endogenous H₂S has been reported detrimental in acute kidney injury caused by nephrotoxic drugs. For instance, the CSE inhibitor PAG (50 mg/kg/day) reduced the kidney damage of Wistar rats induced by cisplatin and adriamycin.[27,28] This is inconsistent with our data in which PAG was unable to relieve renal fibrosis. In fact, 50 mg/kg/day PAG treatment resulted in a great weight loss of normal Sprague–Dawley rats in our study (data not shown), and the dose had to be lowered to 25 mg/kg/day. Such conflicting
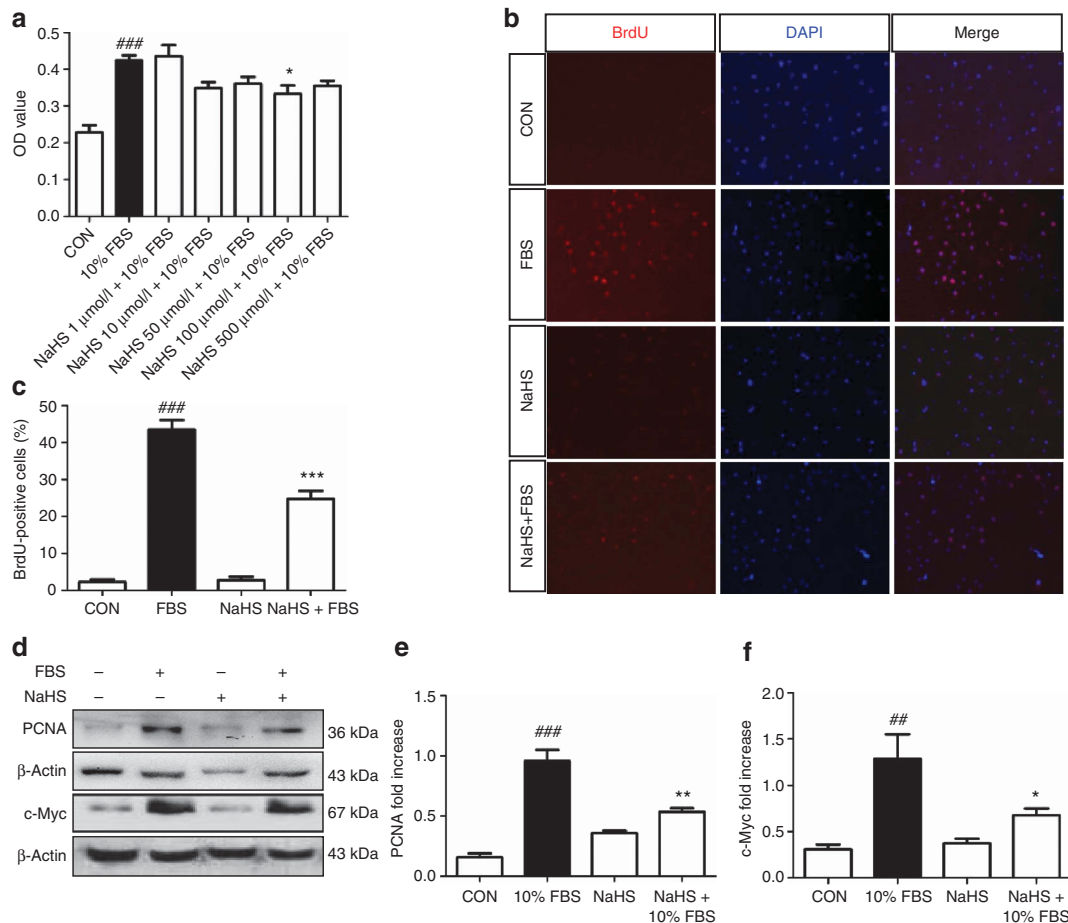
Figure 8 | Sodium hydrosulfide (NaHS) suppresses the proliferation of NRK-49F cells. Serum-starved cells were preincubated with NaHS at concentrations as indicated for 30 min, followed by stimulation with 10% fetal bovine serum (FBS) for 24 h. Serum-starved cells without FBS treatment served as controls (CON). (**a**) MTT (3-(4,5-dimethylthiazol-2-yl)-2,5-diphenyltetrazolium bromide) assay shows the optical density (OD) value of various treatment groups. (**b**, **c**) Representative micrographs (original magnification ×200, **b**) and (**c**) group data display the number of bromodeoxyuridine (BrdU)-positive cells. Cells were stained with anti-BrdU antibody (red) and 4′,6-diamidino-2-phenylindole (DAPI; blue) was used to visualize the nuclei. $N = 6$. (**d–f**) Representative pictures (**d**) and group data analysis (**e**, **f**) for proliferating cell nuclear antigen (PCNA) and c-Myc expressions in NRK-49F cells subjected to various treatments. Relative abundance was determined by normalizing to β-actin. Data are mean ± s.e.m. of three independent experiments. $^{\#\#}P < 0.01$, $^{\#\#\#}P < 0.001$ versus control group; $^*P < 0.05$, $^{**}P < 0.01$, $^{***}P < 0.001$ versus 10% FBS group.

aspects of H₂S implicate that diverse mechanisms of H₂S may exist in different animal models and species. Despite this, caution must be taken in interpreting the effect of PAG because of its nonselective inhibitory action of CSE. It has been reported that D-amino acid oxidase and L-alanine transaminase can also be inhibited by PAG.[29,30] Possibilities cannot be ruled out that the protective effect of PAG in renal disease may be mediated by inactivating other enzymes rather than CSE.

Fibroblast proliferation and phenotypic transition to myofibroblast are two major cellular events of renal fibrosis.[31] FBS contains numerous growth factors that promote the proliferation and differentiation in many types of cells. The effect of H₂S on cell proliferation seems to be cell specific. Some studies reported that H₂S promoted the proliferation in rat intestinal epithelial cells and human colon cancer cells, whereas others demonstrated that it inhibited the

proliferation of lung fibroblasts and pancreatic stellate cells.[32,33] Our data revealed that NaHS at 100 μmol/l not only decreased the cell number, but also inhibited the DNA synthesis stimulated by FBS. These findings were further verified by the fact that NaHS downregulated the expressions of proliferation-related genes including *PCNA* and *c-Myc*. Previous studies also indicated that H₂S induced DNA damage in many cell types.[34] The proliferation and cell cycle proteins such as p53, p21, and cyclin D1 were downregulated by H₂S.[35,36]

Numerous cytokines and growth factors such as TGF-β1, platelet-derived growth factor, tissue plasminogen activator, and plasminogen activator inhibitor-1 are involved in the phenotypic switch of fibroblast to myofibroblast.[37–40] Microarray analysis in an intestinal cell line suggests that TGF-β1 and MAPK kinases are regulated by H₂S.[41] Our results showed that NaHS at 100 μmol/l suppressed mRNA
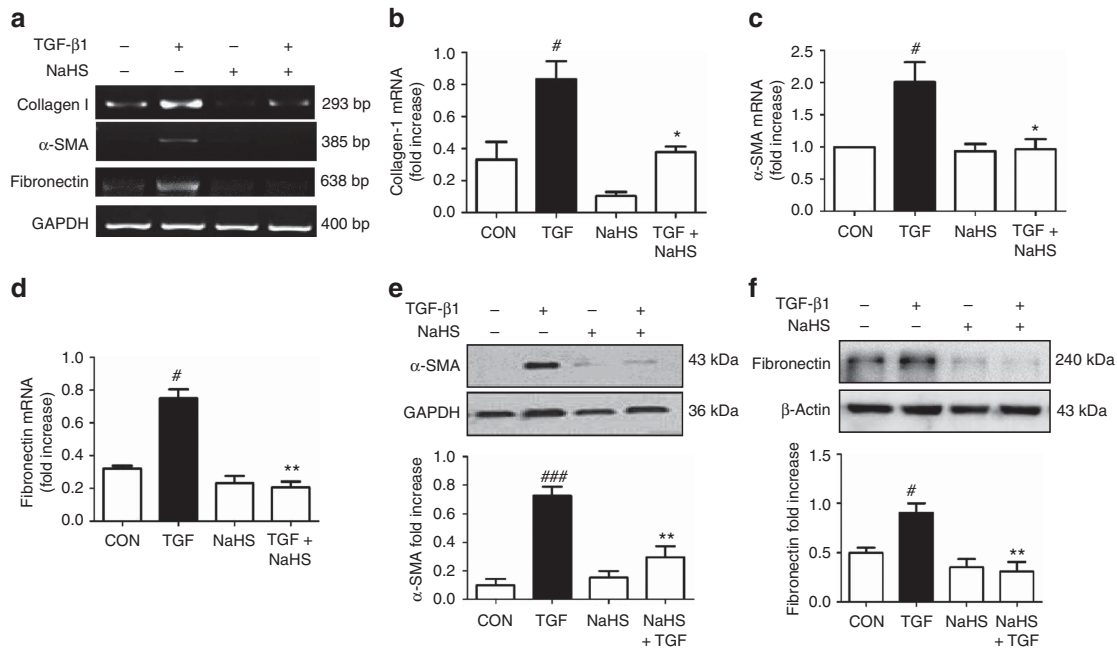
Figure 9 | Sodium hydrosulfide (NaHS) pretreatment blocks the differentiation of renal fibroblasts to myofibroblasts. Serum-starved cells were incubated with NaHS (100 μmol/l) for 30 min, and then stimulated with transforming growth factor-β1 (TGF-β1; 2 ng/ml) for 12 h (reverse transcription–PCR) or 24 h (western blot). (**a–d**) Collagen I, fibronectin, and α-smooth muscle actin (α-SMA) mRNA levels were determined by (**a**) reverse transcription–PCR and (**b–d**) semiquantified by normalizing to glyceraldehyde-3-phosphate dehydrogenase (GAPDH) by densitometric analysis. (**e, f**) Whole-cell lysates were immunoblotted with antibodies against (**e**) α-SMA and (**f**) fibronectin, respectively. GAPDH and β-actin were loaded as internal controls. Data are mean ± s.e.m. of three independent experiments, $^{\#}P<0.05$, $^{\#\#\#}P<0.001$ versus control group; $^{*}P<0.05$, $^{**}P<0.01$ versus TGF group.

and protein expressions of α-SMA and fibronectin induced by TGF-β1. In addition, H$_2$S attenuated the phosphorylation of Smad3, a major pathway in the signal transduction of TGF-β1. These data suggested that H$_2$S inhibited the fibroblast differentiation and extracellular matrix production partially by blocking the TGF-β1-Smad signaling. In addition to Smad-dependent pathway, MAPK kinases also engage in the effect of TGF-β1. ERK, p38, and JNK have been found to be activated in UUO model and regulate the proliferation, migration, and differentiation of fibroblast.[42] Our data indicated that H$_2$S reversed the phosphorylation increase of p38, ERK, and JNK stimulated by TGF-β1 in renal interstitial fibroblasts, implying that the blockade of MAPK kinases activation may be another mechanism responsible for the antifibrotic effect of H$_2$S.

Inflammation plays an important role in the priming and progression of renal fibrosis.[43] One of the pathological features of the UUO rat model is the marked infiltration of inflammatory cells in the renal interstitium. Substantial data support the anti-inflammation action of H$_2$S in multiple organs and systems.[44] Our study echoed with these studies that H$_2$S exhibited an anti-inflammatory property by reducing macrophage recruitment in renal interstitium. The inflammatory cytokines such as interleukin-1β, tumor necrosis factor-α, and monocyte chemoattractant protein-1 were also downregulated by NaHS. MAPKs are involved in modulating inflammatory processes. For example, JNK has been identified with the activation of macrophages and

upregulation of proinflammatory mediators, and JNK inhibition resolves the inflammation.[45] Thus, the anti-inflammatory effect of H$_2$S may be mediated by inhibiting the MAPK signal pathway.

In summary, this study demonstrates for the first time that H$_2$S exhibited antifibrotic effects on obstructed nephropathy and inhibited the proliferation and differentiation of renal fibroblasts both *in vitro* and *in vivo*. The antifibrotic mechanisms of H$_2$S may involve its anti-inflammation as well as its blockade on TGF-β1 and MAPK signaling. This may provide a therapeutic option for renal fibrosis based on H$_2$S modulation. Low dosage of H$_2$S or its releasing compounds may have therapeutic potentials in treating CKD.

MATERIALS AND METHODS
Reagents and antibodies
BrdU, PAG, enalapril, and NaHS, as well as antibodies against PCNA, c-Myc, and BrdU were purchased from Sigma-Aldrich (St Louis, MO). Recombinant human TGF-β1 and Trizol reagent were obtained from Invitrogen (Carlsbad, CA). Antibodies against α-SMA, fibronectin, CBS, and ERK/phosphorylated-ERK were from Santa Cruz Biotechnology (Santa Cruz, CA). CSE antibody was purchased from Abnova Chemical (Taiwan, China). Other antibodies unless specified were from Cell Signaling Technology (Danvers, MA).

Animal surgery and experimental protocols
Male Sprague–Dawley rats (180–200 g) were purchased from Shanghai Laboratory Animal Commission (Shanghai, China).
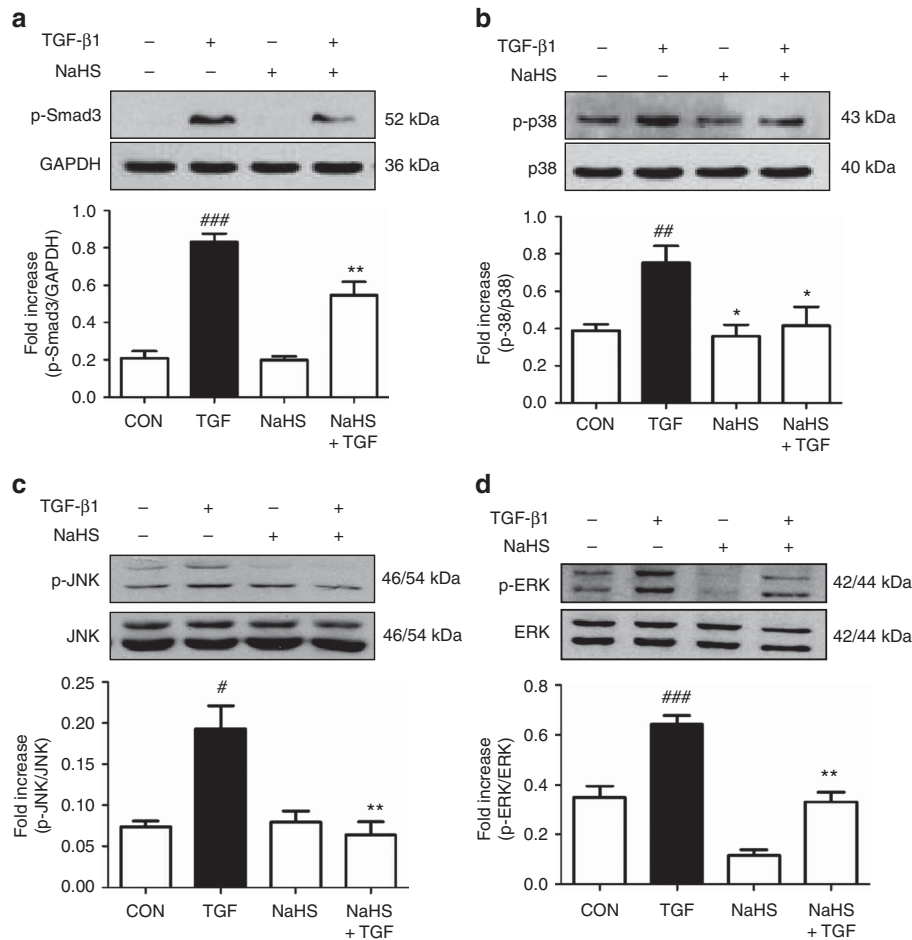
Figure 10 | Sodium hydrosulfide (NaHS) abolishes the phosphorylation increase of mitogen-activated protein kinase (MAPK) and Smad3. Serum-starved cells were incubated with NaHS (100 μmol/l) for 30 min, followed by transforming growth factor-β1 (TGF-β1; 2 ng/ml) treatment for 1 h in the presence or absence of NaHS. Cell lysates were subjected to western blotting with antibodies against (**a**) phospho-Smad3, (**b**) phospho-p38/p38, (**c**) phospho-JNK/JNK, and (**d**) phospho-ERK/ERK. Relative abundance was quantified by densitometry and normalized to glyceraldehyde-3-phosphate dehydrogenase (GAPDH), p38, c-Jun N-terminal kinase (JNK), and extracellular signal–regulated kinase (ERK), respectively. Data are mean ± s.e.m., $n = 3$, $^{\#}P < 0.05$, $^{\#\#}P < 0.01$, $^{\#\#\#}P < 0.001$ versus control group; $^{*}P < 0.05$, $^{**}P < 0.01$ versus TGF group.

UUO operation was performed as described previously.[16] Rats were randomly divided into the following seven groups: sham, UUO, UUO with enalapril (10 mg/kg/day), UUO with three doses of NaHS (5.6, 56, and 560 μg/kg/day), and UUO with PAG (25 mg/kg/day). NaHS and PAG were given intraperitoneally once daily 3 days before surgery and continued for 1 to 2 weeks after operation. Enalapril was given via intragastria. UUO rats received vehicle (saline) treatment. All rats were killed at day 7 or 14 days after surgery. The kidneys were then harvested and plasma was collected accordingly. The experimental protocols were approved by the Institutional Animal Care and Use Committee of Soochow University.

Histological analysis and immunohistochemical staining
Kidney samples were fixed in 10% formalin, embedded in paraffin, and sectioned 4 μm thick. Sections were deparaffined and stained with Masson trichrome reagents and observed under a light microscope. Renal collagen (blue area) was semiquantitatively measured at ×200 magnification in 10 randomly selected fields from 4 animals using Image Pro-Plus 6.0 software (Bethesda, MD).

For immunohistochemical studies, renal sections were incubated with antibodies against α-SMA (1:50), fibronectin (1:50), and CD68 (1:50) overnight at 4 °C, and subsequently incubated with corresponding secondary antibodies at room temperature for 1 h. Peroxidase-Streptavidin-biotin complex (Vector Laboratories, Burlingame, CA) and diaminobenzidine (Sigma, St Louis, MO) was used to visualize the proteins. Ten randomly selected fields (×200 magnifications for α-SMA and fibronectin, and ×400 magnifications for CD68) were photographed and measured by a blinded observer using Image Pro-Plus 6.0 software.

Plasma H₂S and tissue H₂S synthesis measurement
Plasma H₂S level was detected using Dansyl azide (DNS-Az), a novel fluorescent H₂S probe (kindly gifted by Professor Binghe Wang, Georgia State University) as described previously.[24] Briefly, DNS-Az stock solution (2.2 mmol/l) was added at 10 μl per well in a 96-well plate, followed by mixing with 100 μl plasma. Fluorescence was immediately measured by a fluorescent microplate reader (Tecan M200, Grodig, Austria) with an excitation at 360 nm and emission at 528 nm.

Tissue H$_2$S production measurement was performed as previously described.[46] In brief, the left kidney homogenates were mixed with 2 mmol/l pyridoxal 5'-phosphate and 10 mmol/l L-cysteine and 250 µl 10% trichloroacetic acid to reach a total volume of 750 µl. After incubation at 37 °C for 30 min, 250 µl 1% zinc acetate was added to trap H$_2$S. Then, 133 µl of 20 mmol/l N,N-dimethyl-p-phenylenedi-amine sulfate in 7.2 mol/l HCl and 133 µl of 30 mmol/l FeCl$_3$ in 1.2 mol/l HCl were added. The absorbance of the solution was determined at 670 nm with a spectrophotometer. The H$_2$S concentration was calculated against a calibration curve of NaHS (0.1–100 µmol/l).

Cell culture and treatments

Normal rat kidney fibroblasts (NRK-49F) were purchased from American Type Culture Collection (Manassas, VA) and maintained in Dulbecco's modified Eagle's medium (4.5 g/l glucose) supplemented with 10% fetal bovine serum (Gibco, Grand Island, NY). After preincubation with NaHS at various concentrations (1–500 µmol/l) for 30 min, recombinant human TGF-β1 (2 ng/ml) was added for various periods of time. In the control group, cells were treated with vehicle only. In proliferation studies, 10% FBS served as stimulators and the cells were subjected to serum-free medium for 24 h before experimentation.

Cell proliferation assay

Cell proliferation was assessed by MTT assay and BrdU incorporation. For the MTT assay, cells (2×10^3/100 µl) were seeded in 96-well plate until subconfluence and quiescenced with serum-free medium for 24 h. Cells were then pretreated with NaHS (0.1–500 µmol/l) for 30 min, followed by incubation with or without 10% FBS for 24 h. MTT (0.5 mg/ml) was added at 4 h before treatment termination. At the end of treatment, medium was removed and dimethylsulfoxide at 150 µl per well was then added. Absorbance at 490 nm was measured by a microplate reader (Tecan M200).

For the BrdU incorporation, cells were seeded onto coverslips. After being pretreated with 100 µmol/l NaHS for 30 min, cells were incubated in medium with or without 10% FBS for 5 h, and pulsated with BrdU (10 µmol/l) for another 5 h. Next, cells were fixed in 4% paraformadehyde for 20 min and DNA was denatured with 2 N HCl at 37 °C for 10 min. After blocking, the incorporated BrdU was detected with a mouse anti-BrdU antibody (1:100, Sigma) at 4 °C overnight, followed by incubation with Alexa Fluor 555 Donkey anti-mouse IgG (1:500, Invitrogen) for 1 h. Subsequently, coverslips were mounted and observed under a fluorescent microscope (AXIO SCOPE A1; Zeiss, Jena, Germany).

Reverse transcription–PCR and quantitative PCR

Total RNA was extracted with Trizol reagent and reverse transcription–PCR was performed using an Advantage RT-for-PCR kit and PCR Master Mix kit (Fermentas, Vilnius, Lithuania) according to the manufacturer's instructions. The quantitative PCR reactions were performed using a real-time SYBR technology and on ABI Prism 7000 DNA Detection System (Applied Biosystems, Foster, CA). For each sample, glyceraldehyde-3-phosphate dehydrogenase (GAPDH) and 18S RNA was also assayed as an internal control and final result were normalized to and expressed as ratios of the target gene/internal controls. The primers used in the PCR reactions are listed in Supplementary Table S2 online.

Western blot

Given the heterogeneous expression of CBS and CSE in the kidney, the whole kidney was halved in the middle. One half was used for histological studies, and the other half was homogenized for western blotting analysis. Protein samples (20–80 µg) were separated by 8–10% sodium dodecyl sulfate–polyacrylamide gel electrophoresis gels and transferred onto a polyvinylidene difluoride membrane (Millipore, Bedford, MA). After blocking in 5% milk/Tris-buffered saline and Tween-20 buffer, membranes were individually incubated with antibodies against proteins of interest at an appropriate dilution (α-SMA (1:1000), fibronectin (1:500), CBS(1:500), CSE (1:250), ERK/phospho-ERK (1:500), JNK/phospho-JNK (1:500), P38/phospho-P38 (1:500), phospho-Smad3 (1:500), PCNA (1:1000), and c-Myc (1:1000)) at 4 °C overnight. Membranes were then washed and incubated with appropriate horseradish peroxidase–conjugated secondary antibody for 1 h. Visualization was carried out using an advanced chemiluminescence kit (GE Healthcare, Buckinghamshire, UK). The band density was quantified by ImageJ software (Bethesda, MD). GAPDH or β-actin was used as an internal control.

Statistical analysis

All data are presented as mean ± s.e.m. Statistical significance was determined using Student's t-test or one-way analysis of variance followed by a post hoc analysis (Tukey's test) where applicable. The significance level was set at $P < 0.05$.

SUPPLEMENTARY MATERIAL

Table S1. Renal function and serum electrolytes among different animal groups.
Table S2. The primers used for reverse transcription and quantitative PCR reactions.
Supplementary material is linked to the online version of the paper at http://www.nature.com/ki

REFERENCES

1. Harris RC, Neilson EG. Toward a unified theory of renal progression. *Annu Rev Med* 2006; **57**: 365–380.
2. Zeisberg M, Neilson EG. Mechanisms of tubulointerstitial fibrosis. *J Am Soc Nephrol* 2010; **21**: 1819–1834.
3. Boor P, Ostendorf T, Floege J. Renal fibrosis: novel insights into mechanisms and therapeutic targets. *Nat Rev Nephrol* 2010; **6**: 643–656.
4. Boor P, Sebeková K, Ostendorf T et al. Treatment targets in renal fibrosis. *Nephrol Dial Transplant* 2007; **22**: 3391–3407.
5. Wang R. Shared signaling pathways among gasotransmitters. *Proc Natl Acad Sci USA* 2012; **109**: 8801–8802.

6. Xia M, Chen L, Muh RW et al. Production and actions of hydrogen sulfide, a novel gaseous bioactive substance, in the kidneys. *J Pharmacol Exp Ther* 2009; **329**: 1056–1062.

7. Bełtowski J. Hypoxia in the renal medulla: implications for hydrogen sulfide signaling. *J Pharmacol Exp Ther* 2010; **334**: 358–363.

8. Aminzadeh M, Vaziri N. Down-regulation of the renal and hepatic hydrogen sulfide (H₂S) producing enzymes and capacity in chronic kidney disease. *Nephrol Dial Transplant* 2012; **27**: 498–504.

9. Perna AF, Luciano MG, Ingrosso D et al. Hydrogen sulphide-generating pathways in haemodialysis patients: a study on relevant metabolites and transcriptional regulation of genes encoding for key enzymes. *Nephrol Dial Transplant* 2009; **24**: 3756–3763.

10. Sen U, Basu P, Abe OA et al. Hydrogen sulfide ameliorates hyperhomocysteinemia-associated chronic renal failure. *Am J Physiol Renal Physiol* 2009; **297**: F410–F419.

11. Fang L, Li H, Tang C et al. Hydrogen sulfide attenuates the pathogenesis of pulmonary fibrosis induced by bleomycin in rats. *Can J Physiol Pharmacol* 2009; **87**: 531–538.

12. El-Seweidy MM, Sadik NA, Shaker OG. Role of sulfurous mineral water and sodium hydrosulfide as potent inhibitors of fibrosis in the heart of diabetic rats. *Arch Biochem Biophys* 2011; **506**: 48–57.

13. Tan G, Pan S, Li J et al. Hydrogen sulfide attenuates carbon tetrachloride-induced hepatotoxicity, liver cirrhosis and portal hypertension in rats. *PLoS One* 2011; **6**: e25943.

14. Morrissey JJ, Ishidoya S, Mc Cracken R et al. Nitric oxide generation ameliorates the tubulointerstitial fibrosis of obstructive nephropathy. *J Am Soc Nephrol* 1996; **7**: 2202–2212.

15. Wang L, Lee JY, Kwak JH et al. Protective effects of low-dose carbon monoxide against renal fibrosis induced by unilateral ureteral obstruction. *Am J Physiol Renal Physiol* 2008; **294**: F508–F517.

16. Chevalier RL, Forbes MS, Thornhill BA. Ureteral obstruction as a model of renal interstitial fibrosis and obstructive nephropathy. *Kidney Int* 2009; **75**: 1145–1152.

17. Bos EM, Wang R, Snijder PM et al. Cystathionine γ-lyase protects against renal ischemia/reperfusion by modulating oxidative stress. *J Am Soc Nephrol* 2013; **24**: 759–770.

18. Wu N, Siow YL, Karmin O. Ischemia/reperfusion reduces transcription factor SP1 mediated cystathionine b-synthase expression in the kidney. *J Biol Chem* 2010; **285**: 18225–18233.

19. Tripatara P, Patel NSA, Collino M et al. Generation of endogenous hydrogen sulfide by cystathionine gamma-lyase limits renal ischemia/reperfusion injury and dysfunction. *Lab Invest* 2008; **88**: 1038–1048.

20. Lee HJ, Mariappan MM, Feliers D et al. Hydrogen sulfide inhibits high glucose-induced matrix protein synthesis by activating AMP-activated protein kinase in renal epithelial cells. *J Biol Chem* 2012; **287**: 4451–4461.

21. Pan TT, Chen YQ, Bian JS. All in the timing: a comparison between the cardioprotection induced by H2S preconditioning and post-infarction treatment. *Eur J Pharmacol* 2009; **616**: 160–165.

22. Whitfield NL, Kreimier EL, Verdial FC et al. Reappraisal of H₂S/sulfide concentration in vertebrate blood and its potential significance in ischemic preconditioning and vascular signaling. *Am J Physiol Regul Integr CompPhysiol* 2008; **294**: R1930–R1937.

23. Zhong G, Chen F, Cheng Y et al. The role of hydrogen sulfide generation in the pathogenesis of hypertension in rats induced by inhibition of nitric oxide synthase. *J Hypertens* 2003; **21**: 1879–1885.

24. Peng H, Cheng Y, Dai C et al. A fluorescent probe for fast and quantitative detection of hydrogen sulfide in blood. *Angew Chem Int Ed Engl* 2011; **50**: 9672–9675.

25. Wintner EA, Deckwerth TL, Langston W et al. A monobromobimane-based assay to measure the pharmacokinetic profile of reactive sulphide species in blood. *Br J Pharmacol* 2010; **160**: 941–957.

26. Zhang BH, Wu FY, Wu YM et al. Fluorescent method for the determination of sulfide anion with ZnS:Mn quantum dots. *J Fluoresc* 2010; **20**: 243–250.

27. Della Coletta Francescato H, Cunha FQ, Costa RS et al. Inhibition of hydrogen sulphide formation reduces cisplatin-induced renal damage. *Nephrol Dial Transplant* 2011; **26**: 479–488.

28. Francescato HD, Marin EC, Cunha Fde Q et al. Role of endogenous hydrogen sulfide on renal damage induced by adriamycin injection. *Arch Toxicol* 2011; **85**: 1597–1606.

29. Burnett G, Marcotte P, Walsh C. Mechanism-based inactivation of pig heart L-alanine transaminase by L-propargylglycine. Half-site reactivity. *J Biol Chem* 1980; **255**: 3487–3491.

30. Marcotte P, Walsh C. Active site-directed inactivation of cystathionine γ-synthetase and glutamic pyruvic transaminase by propargylglycine. *Biochem Biophys Res Commun* 1975; **62**: 677–682.

31. Liu Y. Cellular and molecular mechanisms of renal fibrosis. *Nat Rev Nephrol* 2011; **7**: 684–696.

32. Fang LP, Lin Q, Tang CS et al. Hydrogen sulfide suppresses migration, proliferation and myofibroblast transdifferentiation of human lung fibroblasts. *Pulm Pharmacol Ther* 2009; **22**: 554–561.

33. Schwer CI, Stoll P, Goebel U et al. Effects of hydrogen sulfide on rat pancreatic stellate cells. *Pancreas* 2012; **41**: 74–83.

34. Baskar R, Bian J. Hydrogen sulfide gas has cell growth regulatory role. *Eur J Pharmacol* 2011; **656**: 5–9.

35. Baskar R, Li L, Moore PK. Hydrogen sulfide-induces DNA damage and changes in apoptotic gene expression in human lung fibroblast cells. *FASEB J* 2007; **21**: 247–255.

36. Yang G, Wu L, Bryan S et al. Cystathionine gamma-lyase deficiency and overproliferation of smooth muscle cells. *Cardiovasc Res* 2010; **86**: 487–495.

37. Böttinger EP, Bitzer M. TGF-beta signaling in renal disease. *J Am Soc Nephrol* 2002; **13**: 2600–2610.

38. Floege J, Eitner F, Alpers CE. A new look at platelet-derived growth factor in renal disease. *J Am Soc Nephrol* 2008; **19**: 12–23.

39. Hao S, Shen H, Hou Y et al. tPA is a potent mitogen for renal interstitial fibroblasts: role of beta1 integrin/focal adhesion kinase signaling. *Am J Pathol* 2010; **177**: 1164–1175.

40. Eddy AA, Fogo AB. Plasminogen activator inhibitor-1 in chronic kidney disease: evidence and mechanisms of action. *J Am Soc Nephrol* 2006; **17**: 2999–3012.

41. Deplancke B, Gaskins HR. Hydrogen sulfide induces serum-independent cell cycle entry in nontransformed rat intestinal epithelial cells. *FASEB J* 2003; **17**: 1310–1312.

42. Ma FY, Sachchithananthan M, Flanc RS et al. Mitogen activated protein kinases in renal fibrosis. *Front Biosci (Schol Ed)* 2009; **1**: 171–187.

43. Lee SB, Kalluri R. Mechanistic connection between inflammation and fibrosis. *Kidney Int Suppl* 2010; **78**: S22–S26.

44. Wallace JL, Ferraz JG, Muscara MN. Hydrogen sulfide: an endogenous mediator of resolution of inflammation and injury. *Antioxid Redox Signal* 2012; **17**: 58–67.

45. Kyriakis JM, Avruch J. Mammalian MAPK signal transduction pathways activated by stress and inflammation: a 10-year update. *Physiol Rev* 2012; **92**: 689–737.

46. Hu LF, Lu M, Tiong CX. Neuroprotective effects of hydrogen sulfide on Parkinson's disease rat models. *Aging Cell* 2010; **9**: 135–146.